CrossMark

RESEARCH PAPER

Preparation, characterization, and in vitro activity evaluation of triblock copolymer-based polymersomes for drugs delivery

Lucas N. Besada · Pablo Peruzzo · Ana M. Cortizo · M. Susana Cortizo

Abstract Polymersomes are polymer-based vesicles that form upon hydration of amphiphilic block copolymers and display high stability and durability, due to their mechanical and physical properties. They have hydrophilic reservoirs as well as thick hydrophobic membranes; allowing to encapsulate both water-soluble bioactive agent and hydrophobic drugs. In this study, poly ethylene glycol (PEG3350 and PEG6000) were used as hydrophilic part and poly(vinyl benzoate) (PVBz) as hydrophobic block to synthesize amphiphilic triblock copolymers (PVBz-*b*-PEG-*b*-PVBz). Different proportions of hydrophilic/hydrophobic part were assayed in order to obtain polymersomes by solvent injection method. For the synthesis of the copolymers, the initial block of PEG was derived to obtain a macroinitiator through a xanthate functional group (PEGX3 or PEGX6) and the polymerization of vinyl benzoate was carried out through reversible addition-fragmentation chain transfer polymerization (RAFT). The structure of PEGX and copolymers was confirmed by Infrared, ^{1}H-NMR and UV-Vis spectrometry, while the average molecular weight (M_w) and polydispersity index (PI) were determined by size exclusion chromatography (SEC). The structures adopted by the copolymers in aqueous solution by self-assembly were investigated using transmission electron microscopy (TEM), dynamic light scattering (DLS) and small-angle X-ray scattering (SAXS). Both techniques confirm that polymersomes were obtained for a fraction of hydrophilic block (f) $\approx 35 \pm 10\%$, with a diameter of 38.3 ± 0.3 nm or 22.5 ± 0.7 nm, as determined by TEM and according to the M_w of the precursor block copolymer. In addition, we analyzed the possible cytotoxicity in view of its potential application as biomedical nanocarrier. The results suggest that polymersomes seem not induce cytotoxicity during the periods of time tested.

L. N. Besada · A. M. Cortizo
Laboratorio de Investigaciones en Osteopatías y Metabolismo Mineral (LIOMM), Departamento de Cs. Biológicas, Facultad de Cs. Exactas, UNLP, La Plata, Argentina

L. N. Besada · P. Peruzzo · M. S. Cortizo
Instituto de Investigaciones Fisicoquímicas Teóricas y Aplicadas (INIFTA), Dpto. de Química, Fac. Cs. Exactas, UNLP, CCT- La Plata, CONICET CC 16, Suc. 4., La Plata, Argentina

M. S. Cortizo (✉)
La Plata, Argentina

Introduction

The past decade has been a dramatic increase in research into the use of polymer self-assembled nanostructures to drug deliver and regenerative medicine (Pippa et al. 2016; Li and Tan 2014). Both, polymeric vesicles and micelles had been obtained by nanostructuration of amphiphilic block copolymers which demonstrated

Springer

versatile properties in drug delivery and pharmaceutical applications (Lee and Feijen 2012; Alibolandi et al. 2015). These delivery systems will allow effective transport and release at the site of action; overcome the disadvantages associated with direct drugs administration: immune system activation, short half-life, low solubility, and rapid kidney clearance (Harris and Chess 2003).

The advances in novel-controlled polymerization techniques have allowed the design of a wide variety of amphiphilic block copolymers which can self-organize into nanostructures with diverse morphologies, between the micelles, rods, lamellae, tubulus, and vesicles (Mai and Eisenberg 2012). The kind of morphology obtained is determined by the fractions of hydrophilic block (f). It is considered as unifying rule, that polymersomes are generated when $f \approx 35 \pm 10\%$, while $f > 45\%$ and $f < 25\%$ can be expected to form micelles and inverted microstructures, respectively (Discher and Ahmed 2006). Polymersomes which exhibit a phospholipid-like ratio but much larger molecular weight, display higher stability and durability due to their mechanical and physical properties, in comparison to liposomes. These characteristics have promoted the growing development of new multiblock amphiphilic copolymers including other interesting properties such as pH, UV light, or redox sensitivity and biodegradability (LoPresti et al. 2009). As drug nanocarriers, polymersomes have many advantages over the classical lipid liposomes including adequate stability, long circulation in bloodstream, lower premature drug release, and great potential for advanced chemical functionalization (Christian et al. 2009; Discher and Eisenberg 2002; Meng and Zhong 2011; Blanazs et al. 2009). In comparison with polymeric micelles or other solid spherical nanoparticles that are usually used as the vehicles of hydrophobic drugs, polymersomes have hydrophilic reservoirs as well as thick hydrophobic membranes; they can thus encapsulate both water-soluble bioactive agent and hydrophobic drugs for combinatorial therapeutics (Blanazs et al. 2009; Brinkhuis et al. 2011; Onaca et al. 2009).

For many years, polyethylene glycol (PEG) has been widely used as the hydrophilic material to be employed in the synthesis of polymersomes. PEG inhibits the uptake and clearance of colloidal particles by reticulo-endothelial system, increases the blood circulation time of these carriers (Mosqueira et al. 2001; Woodle 1995), shows little toxicity, and lacks immunogenicity

(Working 1997), and the elimination from the body is carried out by either the kidneys (for PEG < 30 kDa) or in the feces (for PEG < a 20-kDa) (Yamaoka et al. 1994). The FDA (Food and Drug Administration) has approved PEG for use as a vehicle or base in food, cosmetics and pharmaceuticals, including injectable, topical, rectal and nasal formulations.

On the other hand, it has been reported that poly (vinyl benzoate) (PVBz) is a biodegradable and non-toxic hydrophobic polymer (Labruère et al. 2010). It was proved that nanoparticles based on PVBz are very slowly degraded in vitro via side chain hydrolysis to release benzoic acid and poly(vinyl alcohol), PVA; both byproducts could be metabolized in vivo. PVA was approved by the FDA for several uses and clinical application in human (Davidson and Terbrugge 1995). Very few block copolymers, including PVBz block were previously prepared. Lipscomb and col., described the syntheses of block copolymers derived from vinyl ester monomers, including PVBz, using xanthate-mediated RAFT polymerizations and analyzed the state-solid morphologies and mechanical properties of these materials (Lipscomb and Mahanthappa 2009, 2011). PVAc-b-PVBz diblock copolymers were obtaining by RAFT polymerization under microwave heating conditions (Roy and Sumerlin 2011). In none of these works, the self-assembly behavior in solution of the synthetized block copolymer was studied.

Based on this background, in this study, amphiphilic triblock copolymer (PVBz-b-PEG-b-PVBz) with different hydrophilic/hydrophobic ratio was synthesized. For some copolymers, selected based on its f, the morphology of the nanostructures obtained by self-assembly was analyzed. In addition, we examined the possible cytotoxicity in view of its potential application as biomedical nanocarrier.

Materials and methods

Materials

Two samples of poly(ethylene glycol), (PEG) were used in this work in order to obtaining the macro-chain transfer agents (CTA) to carry out the RAFT polymerization. PEG$_{3350}$ was donated by Dominguez Laboratory S.A. and PEG$_{6000}$ ($\geq 99\%$) was purchased from BioPaCK. Benzoyl peroxide (BP, Merck-Argentina), was recrystallized from methanol. Vinyl Benzoate (VBz, 99%)

monomer was supplied by Aldrich and purified by distillation under reduced pressure before use. Other solvents and reagents were supplied by Sintorgan and BioPack and used as received.

Synthesis of PEG macro-CTA

For the synthesis of PEG macro-CTA (PEGX), a round-bottomed flask was charged with PEG_{3350} (4 g; 0.12 M) or PEG_{6000} (8 g; 0.13 M) and toluene (10 ml). The flask was heated to 30 °C and the toluene evaporated at reduced pressure to remove residues of water present in the PEG. Then, the flask was charged with toluene (25 ml), KOH (0.15 g; 0.11 M), and dibenzo-18-crown-6 (18-C-6, 0.01 g; 0.001 M) and placed in a preheated silicon bath at 60 °C for 24 hs. The resulting solution was cooled to 30 °C, S_2C (0.15 mL, 0.1 M) was slowly added, and left overnight. To this system, 0.34 ml (0.1 M) of ethyl 2-bromopropionate were added and allowed to stand 24 hs. After which, the solution was filtered and 10 ml dichloromethane was transferred to organic phase. To remove the unreacted polyethylene glycol, two extractions were made with ammonium chloride solution (w/v%) and finely centrifuged to phase's separation. The organic phase was dried by anhydrous sodium chloride and then precipitated in cold diethyl ether/petroleum ether (50/50 V/V). Macro-CTA agent was centrifuged and dried at constant weight in vacuum at room temperature for evaluation of the yield of the reaction.

Synthesis of poly(vinyl benzoate)-*b*-poly(ethyleneglycol)-*b*-poly(vinyl benzoate) by RAFT polymerization

The PVBz-*b*-PEGX-*b*-PVBz triblock copolymers were prepared by reversible addition-fragmentation chain transfer (RAFT) polymerization. Here, X corresponds to the PEG precursor: 6 or 3 for PEG_{6000} or PEG_{3350}, respectively. A solution containing PEGX macro-CTA (5.62 mM), vinyl benzoate (3.61 M), and benzoyl peroxide (BP, 1.32 mM) in toluene (60 wt%) was added to a Schlenk tube. The reactants were degassed via three freeze-pump-thaw cycles and placed in a water bath at 70 °C for different times. The solution was precipitated in cold hexane and the copolymer was purified by dissolution in chloroform and precipitation in cold hexane. Then, the copolymer was centrifuged and dried at

constant weight in vacuum at room temperature for conversion estimation.

Characterization methods

Fourier transform infrared spectra (FTIR) of the polymer films deposited onto a sodium chloride (NaCl) window were recorded on a Nicolet 380 FTIR (Thermo Electron Corporation, Madison WI, USA) between 4000 and 400 cm^{-1} with a resolution of 4 cm^{-1} and 32 scans of accumulation. The EZ-OMNIC software was used to analyze the spectra.

^{1}H-NMR spectra of polymers were recorded with aVariam-200 MHz (Mercury 200) at 35 °C in chloroform-d1. Tetramethylsilane was used as an internal standard.

UV-visible absorption spectra were obtained with a PG instrument T60 UV-Vis spectrophotometer with 1 cm optical path cell using chloroform spectroquality as solvent. These measurements were used to characterized the UV absorption band of the C=S in the structure of the PEGX macro-CTA.

The molecular weight distribution and the average molecular weights were determined by size exclusion chromatography (SEC) in a LKB-2249 instrument at 25 °C. A series of μ-Styragel columns in the pore size range 10^5, 10^4, 10^5, and 100 Å were used, with chloroform as an eluent. The sample concentration was 4–5 mg/mL and the flow rate was 0.5 mL/min. The polymer was detected by UV detector (Shimadzu SPD-10A) and the calibration was done with polystyrene standard. The fraction of hydrophilic block (*f*) was estimated from the PEGX and triblock copolymer M_n relationship.

Self-assembly of triblock copolymers

For the polymersomes preparation, a stock THF solution of PVBz-*b*-PEG6-*b*-PVBz (10 mg/ml) or the PVBz-*b*-PEG3-*b*-PVBz (5 mg/ml) were prepared. Then, 10 ml of milliQ water were dripped in 1 ml of polymer solution with a flow of 30 ml/hs under 600 rpm magnetic agitation at room temperature. Alternatively, ferrocene-loaded polymersomes were prepared following the same procedure, including the addition of 0.3 mg/ml of ferrocene in the initial THF polymer solution.

Characterization of polymersomes

Transmission electron microscopy (TEM) was performed with a JEOL 1200 EX II microscope. The sample was adsorbed onto the copper grids and negatively stained with 0.5% (wt/v) phosphotungstic acid adjusted to pH 7.

The mean diameter and size distribution (PDI) were measured by dynamic light scattering (DLS) (Nano ZS Zetasizer-ZEN3600, Malvern Instruments Corp., UK) provided with a 4-mW He-Ne (633 nm) laser, in water at 25 °C. Data was analyzed using CONTIN algorithms (Malvern Instruments) and the results are expressed as the average of six measurements.

Small-angle X-ray scattering (SAXS) measurements of samples were performed at the D02A-SAXS2 beamline at the Brazilian Synchrotron Light Laboratory (LNLS, Campinas, SP, Brazil), using a monochromatic X-ray beam with a wavelength of $\lambda = 1.544$ Å. The samples were placed between two mica sheets. Polymersomes unload or load with ferrocene, in order to enhance the electronic contrast, were analyzed (Johnston et al. 2010). The collimated X-ray beam was passed horizontally through a chamber containing the sample. The scattering spectrum was collected on a marCCD detector placed at a distance of 3061.3 mm from the sample, covering a scattering vector q ranging from 0.04 to 1.45 nm^{-1}. Scattering intensity was measured as a function of the magnitude q of the scattering vector given as $q = 4\pi \sin\theta/\lambda$, where 2θ being the scattering angle and λ the X-ray wavelength. The experimental intensities were corrected for contribution for the solvents and empty cell. Measurements were performed at 25 °C with an exposure time of 300 s. Experimental data were analyzed using the NCNR SANS/USANS Package based on Igor Pro software (Kline 2006).

RAW264.7 macrophages culture, incubations, and cytotoxicity studies

Murine macrophage RAW 264.7 cells were grown in DMEM (Invitrogen, Buenos Aires, Argentina) containing 10% FBS (Natacor, Argentina), 100-U/ml penicillin and 100 mg/ml streptomycin at 37°C in a 5% CO$_2$ atmosphere.

The influence of polymersomes on the cell viability was tested using 3-(4,5-dimethylthiazol-2-yl)-2,5-diphenyl tetrazolium bromide (MTT) assay (Lastra et al. 2017). RAW 264.7 cells were plated in 24-well

plate using 10% FBS-DMEM in a humidified atmosphere of 95% air and 5% CO$_2$ and incubated for 24 hs. The medium was aspirated and replaced by a medium without phenol red and supplemented with 1% FBS. This assay measures the reduction of the tetrazolium salt MTT to formazan by intact mitochondria in living cells. Thus, absorbance change is directly proportional to the number of viable cells. The effect of the polymersomes was evaluated at two concentrations, 10 and 50 μg/ml and cells were cultured during 48 hs. These concentrations were chosen based on previous references and they could be relevant for future biological applications (Liu et al. 2010; Colley et al. 2014). After these culture periods, cells were incubated for two additional hours with a solution of 0.1 mg/mL MTT. After washing, the formazan precipitate was dissolved in dimethyl sulfoxide (DMSO) and the absorbance read at 570 nm.

Statistical analysis

Student's t test was used for comparisons between the control and experimental groups. All results are expressed as mean ± SEM and represent at least three different experiments performed in triplicate.

Results and discussion

PEG macro-CTA and triblock copolymers

PEG macro-CTAs (PEG6 or PEG3) were synthesized according to the reaction sequence shown in Scheme 1, and characterized by spectroscopic measurements. In both cases, the increase in the UV absorbance confirms the inclusion of the xanthate group on the PEG structure.

PEG6. Yield 42%. FTIR (ν, cm^{-1}) 2948, 2877 (C–H), 1734 (>C=O), 1114 (C–O), 1060 (>C=S), 843 (>C–S). ^{1}H-NMR (CDCl$_3$):(δ, ppm), 4.63 (CH$_3$–CH$_2$–OC(O)), 4.40 (>CH–CH$_3$), 4.23 (–CH$_2$–OC(S)), 3.60–3.85 (–CH$_2$–CH$_2$–O), 1.60 (>CH–CH$_3$), 1.30 (CH$_3$–CH$_2$–OC(O)). UV(>C=S), CHCl$_3$: ($\pi \rightarrow \pi^*$, $\lambda_{max} = 280$ nm) and ($n \rightarrow \pi^*$, $\lambda_{max} = 357$ nm).

PEG3. Yield 43%. FTIR (ν, cm^{-1}) 2950, 2872 (C–H), 1732 (>C=O), 1107 (C–O), 1057 (>C=S), 840 (>C–S). ^{1}H-NMR (CDCl$_3$):(δ, ppm), 4.69 (CH$_3$–CH$_2$–OC(O)), 4.38 ((>CH–CH$_3$), 4.20 ((–CH$_2$–OC(S)), 3.60–3.82 (–CH$_2$–CH$_2$–O), 1.58 (>CH–CH$_3$), 1.27
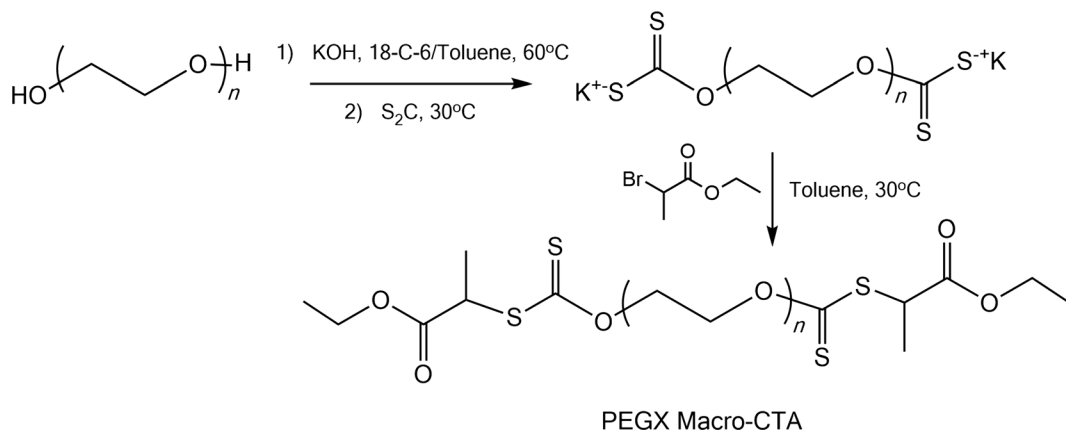
Scheme 1 Synthesis of PEGX macro-CTA

(CH_3–CH_2–$OC(O)$). UV(>C=S), $CHCl_3$: ($\pi \rightarrow \pi^*$, $\lambda_{max} = 280$ nm) and ($n \rightarrow \pi^*$, $\lambda_{max} = 357$ nm).

Both macro-CTA were used for synthesized block copolymers including different composition of PVBz, through RAFT polymerization, as represented in Scheme 2.

This kind of triblock copolymer has been previously synthesized starting of other xanthate macro-CTA under a little different experimental condition; however, the self-assembly in solution of these materials was not studied (Lipscomb and Mahanthappa 2011). We are interesting in analyzed the effect of the average molecular weight on the morphologies obtained by self-assembly of theses copolymers. All samples were identified by ^{1}H-NMR and Fig. 1 shows a representative spectrum together with the corresponding assignation.

Table 1 presents the characteristic of the samples prepared. In the first place, we optimize the reaction conditions, changing the reaction times. As can be seen in the table, for sample 1 prepared from PEG6, after 4.5 h the conversion of the reaction was low and the hydrophilic mass fraction (f) was 67%, suggesting a slow growth of the PVBz block. When the reaction time increased at 17 h (sample 2), the percent of conversion and f attained 26.4 and 42%, respectively. On the other hand, the block copolymers synthesized starting of PEG3 at similar times, lead to good yield of reaction (samples 3 and 4), while for these samples, the f values were 48 and 31%, respectively.

Reaction conditions: [VBz]:[PEGX]:[BP] = 642:1:0.24 in 60 wt% solution in toluene at 70 °C. M_n and M_w/M_n were determined using SEC with

Scheme 2 Synthesis of Poly(vinyl benzoate)-b-poly(ethyleneglycol)-b-poly(vinyl benzoate) triblock copolymers by RAFT polymerization
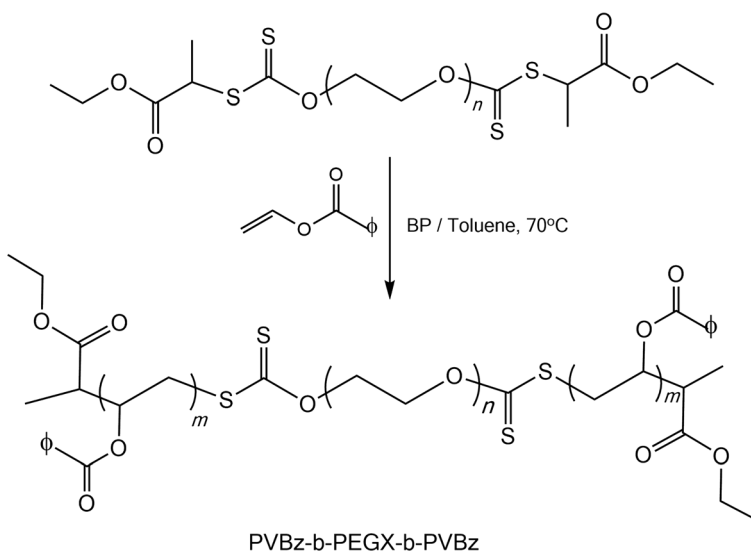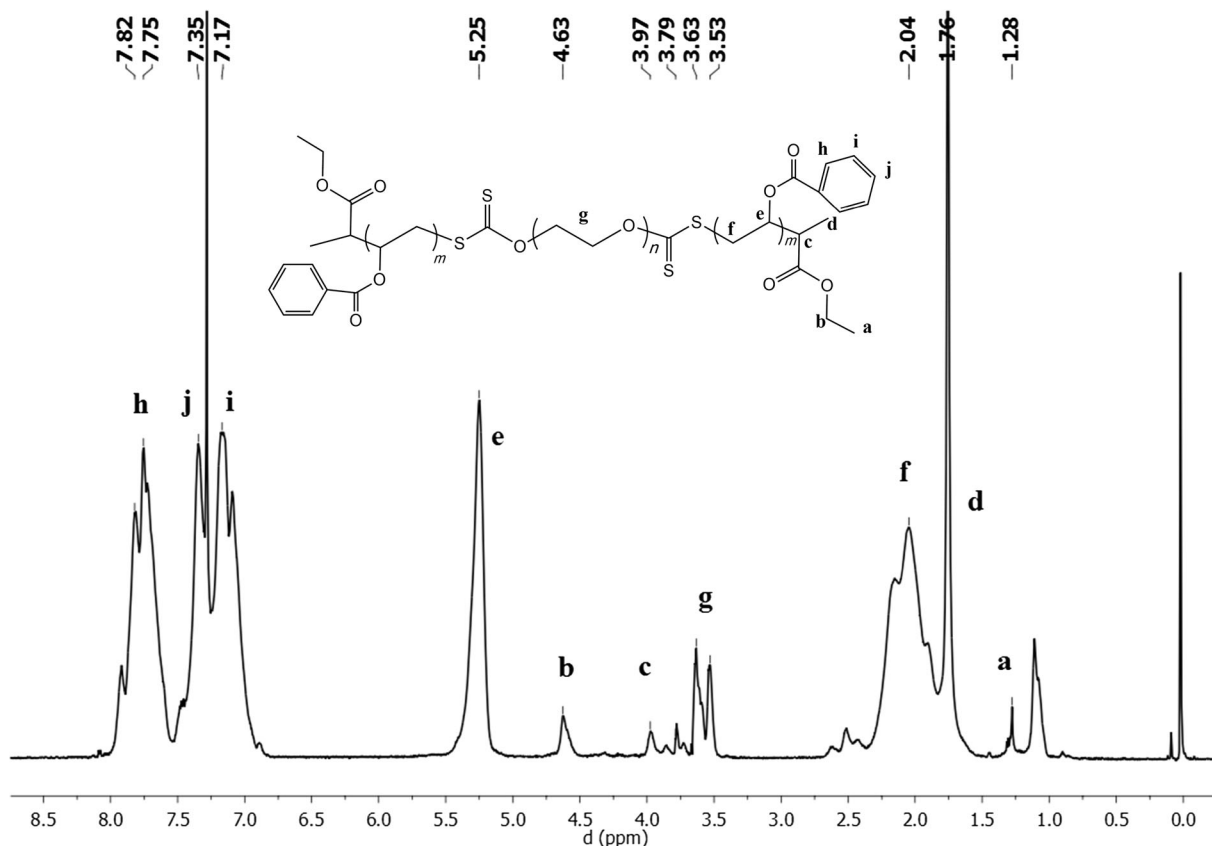
**Fig. 1** ^{1}H-NMR spectrum of PVBz-*b*-PEGX-*b*-PVBz triblock copolymer

polystyrene standard calibration. *f* = hydrophilic fraction mass percentage.

The number-average molecular weight (M_n) and the polydispersity index (M_w/M_n) were analyzed by SEC in chloroform as eluent and calculated based on polystyrene standard. Figure 2a, b shows the change on the M_n in relationship to the PEGX precursor. The M_n value obtained for both PEG6 and PEG3 are highest than the corresponding to initial polyethylenglycol (6.0 and 3.3 Kg/mol) and these differences can be attributed to that the size exclusion chromatography is a relative method which analyzes the average molecular

weight and the molecular weight distribution based on the hydrodynamic volume of the macromolecules. The relationship between this parameter and the average molecular weight is not direct but dependent of a calibration curve built with polymer standard, so they are apparent values. However, the changes shown in Fig. 2a, b allow to appreciate the increase on the M_n with the increased of the reaction conversion, which is an evidence of the RAFT polymerization mechanism. Besides, the increase in the molecular size of PVBz block allows obtaining different *f* values, which will allow us select the adequate block copolymers for

Table 1 Vinyl benzoate RAFT copolymerization

Sample	Precursor	M_n(PEGX), Kg/mol	M_w/M_n	time, hs	%Conv	M_n(final), Kg/mol	M_w/M_n	*f*, %
1	PEG6	8.33	1.20	4.5	2.0	12.50	1.78	67
2	PEG6	8.33	1.20	17	26.4	20.00	2.70	42
3	PEG3	4.02	1.31	17	11.6	8.34	1.70	48
4	PEG3	4.02	1.31	19	14.7	12.95	1.86	31
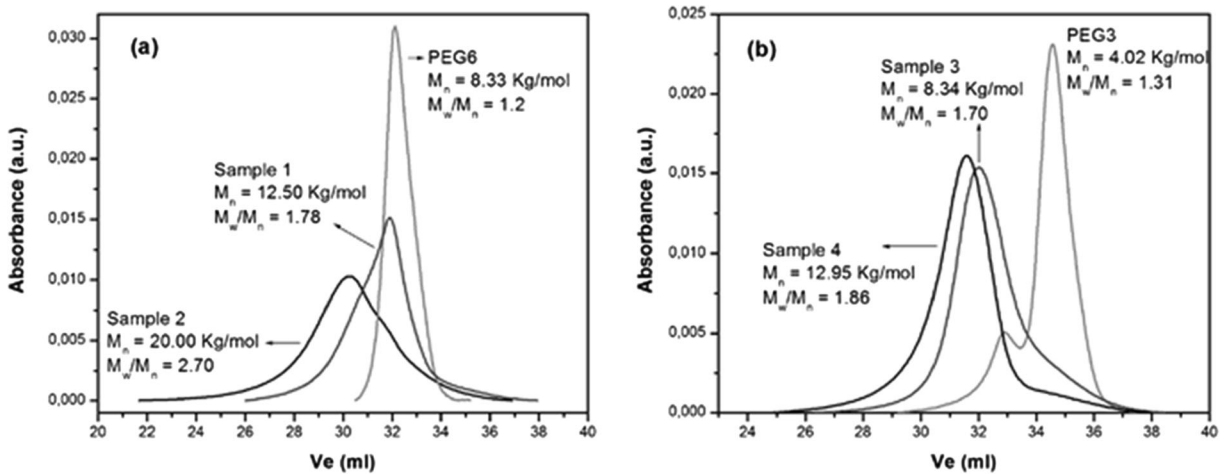
Fig. 2 Chromatographic profiles of triblock copolymers synthesized starting of PEG6 (**a**) and PEG3 (**b**) by RAFT polymerization. Reaction conditions: [VBz]:[PEGX]:[BP] = 642:1:0.24 in 60 wt% solution in toluene at 70 °C

prepared polymersomes by self-assembly, as will be discussed in the next section.

Self-assembly of triblock copolymers

Base on the results present in Table 1, triblock copolymers with different M_n and f values were obtained. Figure 3 shows the TEM image of the morphology (a and c) obtained from self-assembly of samples 2 and 4, as well as the corresponding size distribution (b and d). It is possible to see that both triblock copolymers obtained from PEG6 ($f = 42$) and PEG3 ($f = 31$) can be organized in polymersomes of 38.3 ± 0.3 nm and 22.5 ± 0.7 nm average diameter and narrow distribution. Samples 1 and 3, as was expected, do not form homogeneous and monodisperse polymersomes (see online resource).

The intensity size distribution curves obtained for dynamic light scattering (DLS) of samples 2 and 4 is presented in Fig. 4. Sample 2 shows a monomodal distribution with a hydrodynamic Z-average diameter (Z_D) of 119 ± 1 nm and polydispersity index (PDI) of 0.17, which indicated a narrow size range. Instead, sample 4 exhibits two intensity populations, one of them at lowest size ($Z_D = 57 \pm 2$ nm) and other at the highest size ($Z_D = 408 \pm 18$ nm). This last population could be attributed to few larger aggregates which scatter significantly more, due to the intensity of Rayleigh scattering, (I) is related with the particle diameter (d) as I~d^6 (Habel et al. 2015). On the other hand, differences were observed between the particle size of both samples as measure by TEM or DLS 38.3 ± 0.3 nm or 119 ± 1 nm for sample 2 and 22.5 ± 0.7 nm or 57 ± 2 nm for samples

2 and 4, respectively. These results are not surprising because of a light scattering technique measure hydrodynamic diameter, usually in aqueous medium, and thus due to the hydrophilic crown of the polymersomes (PEG in our cases) the diameter could be four–five times larger than the value determined by TEM, as it was previously demonstrated in other research (Johnston et al. 2010; Habel et al. 2015).

Small-angle X-ray scattering (SAXS) is an analytical technique used in the structural characterization of materials of nanometric size which allows obtaining information on particle size, morphology, and internal structure (Zelikin et al. 2010). In this work, we applied this methodology to reach deeper information about the nanostructures obtained from the triblock copolymers. Figure 5a, b shows the SAXS curves for polymersomes of samples 2 and 4, with or without ferrocene, S2 or S2/F and S4 or S4/F, respectively. This type of scattering is compatible with the presence of the vesicles observed by TEM (García-Juan et al., 2016; Lopez-Oliva et al. 2015). At low q values, a typical linear slope is observed in the log-log plot, with the intensity following a power law of q^{-2} according to Guinier's law (see inset graphs) (Guinier and Fournet 1955). In this zone, it is possible to evaluate the radius of gyration due to the scattered intensity which depends directly on this parameter through the following approximation:

$$I(q) \cong I_0 \left[\frac{-q^2 R_g^2}{3} \right] \tag{1}$$
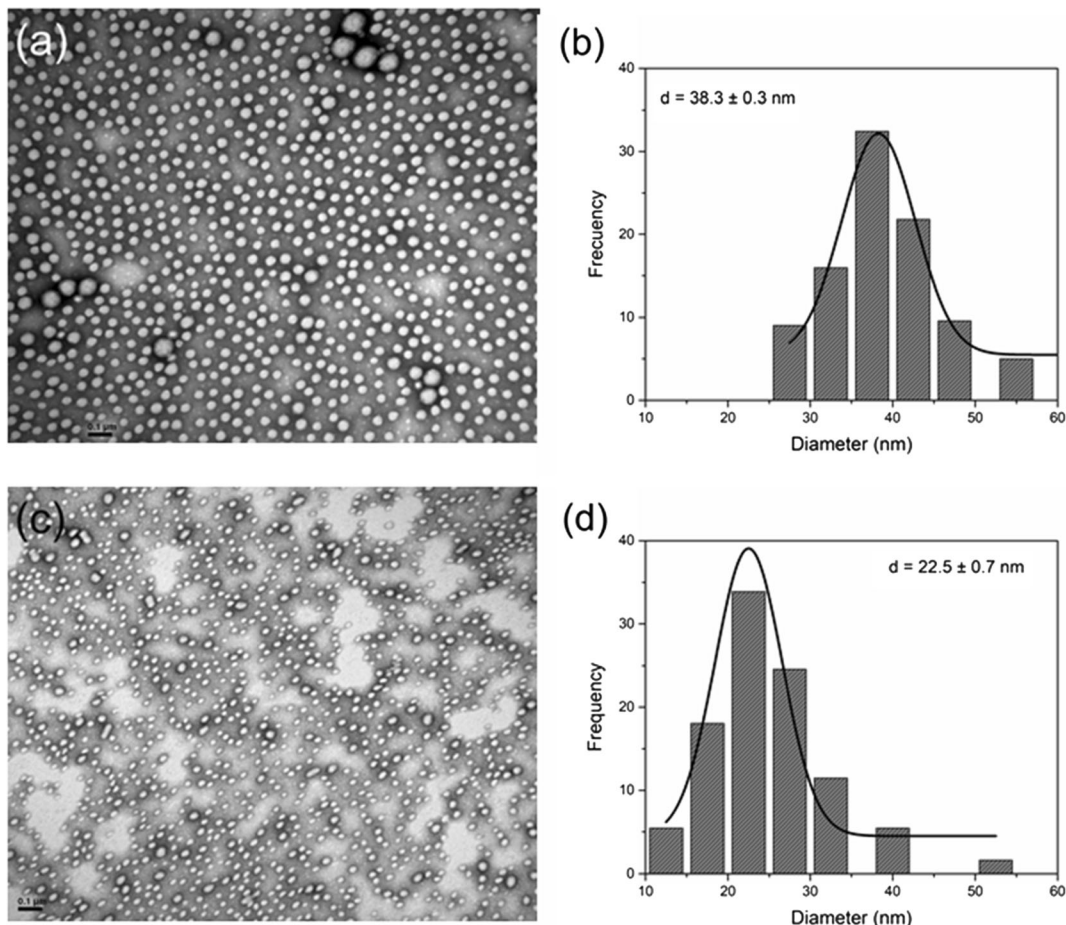
Fig. 3 Transmition electron microscopy (TEM) micrographs of the morphologies formed from samples 2 (**a**) and 4 (**c**), and the corresponding size distribution of polymersomes (**b** and **d**, respectively)
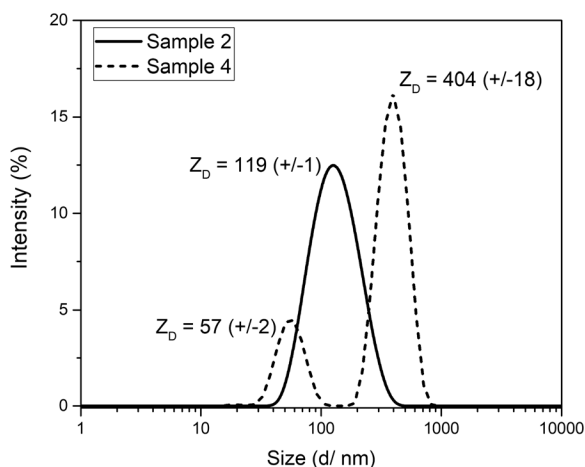

Fig. 4 Particle size distribution of polymersomes based on intensity graphs. Samples 2 (solid line) and 4 (dash line). Z_D is the hydrodynamic Z-average diameter for each population

where I_0 is the intensity to zero angle and R_g is the radius of gyration. So, plots of ln $I(q)$ vs q^2 were presented in the insert of Fig. 5a, b. Guinier's plots show a tendency to an aggregation behavior based on the positive deviation observed at low q. From the linear region, they allow us to obtain the following values for R_g, 18.5 and 15.0 nm for the polymersomes prepared of samples 2 and 4, respectively. In addition, ferrocene-loaded samples showed a contribution at q around 0.03 Å^{-1} related to an increase in the electronic contrast in the samples due to the accumulation of this component inside the hydrophobic layer of the polymersomes wall (Johnston et al. 2010). This contribution allowed defining a SAXS profile in agreement with a vesicular morphology.

The middle q region of the ferrocene-loaded samples were correlated with the calculated scattering from a polydisperse spherical shell particle, where the shell (with constant thickness) has a Gaussian profile of the
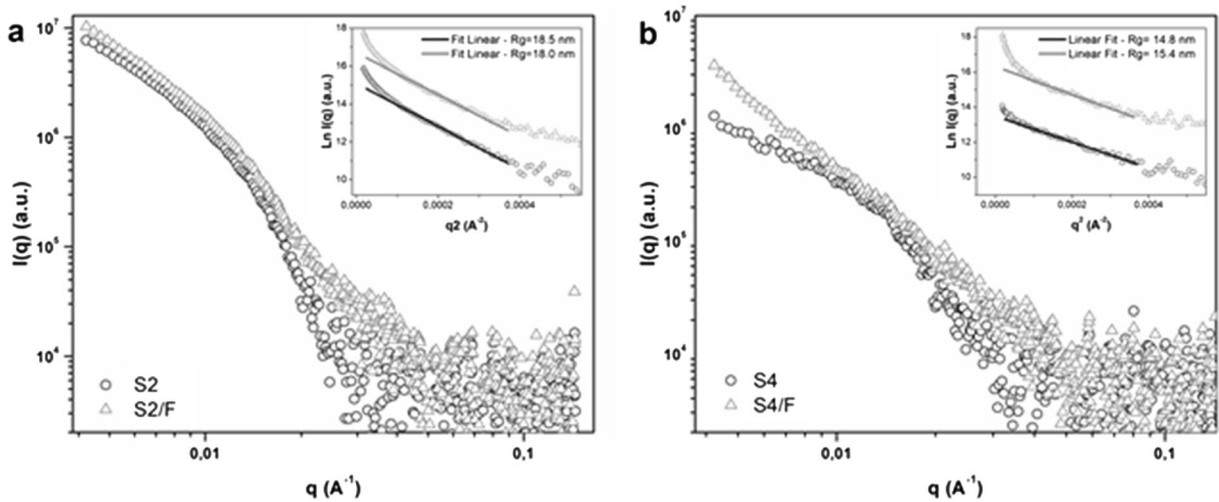
Fig. 5 SAXS curves of nanostructures obtained from samples 2 and 4 (**a** and **b**) unloaded or loaded with ferrocene (S2 and S4 or S2/F and S4/F). Insert: Guinier's plots

scattering length density distributed around the shell radius r_0 (from the center of the particle at the center of the shell) (Gradzielski et al. 1995). The scattering curves obtained from the fit performed using the NCNR SANS/USANS Package based on Igor Pro software are shown in Fig. 6. From the analysis, we obtained $r_0 = 8.6$ nm, $\sigma = 0.4$, and $t = 3$ nm for S2/F sample, and $r_0 = 7.4$ nm, $\sigma = 0.5$, and $t = 1.5$ nm for S4/F sample where σ and t are the radius polydispersity and the shell thickness parameter of the Gaussian function for the scattering length density of the shell, respectively. Calculating the thicknesses for a shell model with sharp boundaries,
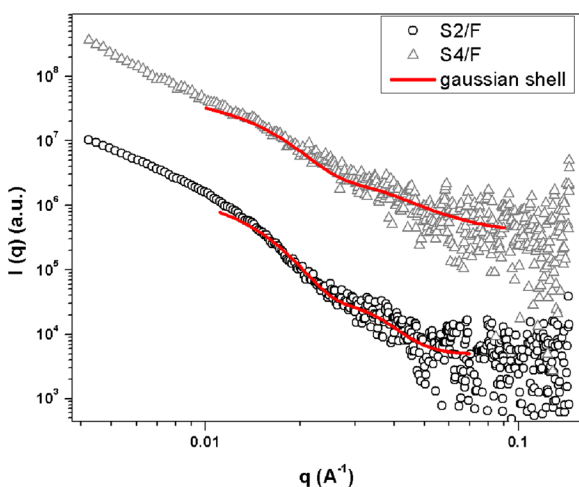
δ, from the parameter t, we found $\delta = 7.5$ nm and $\delta = 3.7$ nm for S2/F and S4/F, respectively. Thus, the SAXS results indicate that the obtained particles are vesicles, while S2/F has vesicles with a particle diameter d 26 nm and a wall thickness t_w 7 nm, S4/F has smaller and more polydisperse vesicles with d 19 nm and t_w 4 nm, in good agreement with TEM results. In addition, the obtained δ values of the samples are consistent with the molecular weight of the polymers from which they were obtained, where the polymer with higher molecular weight lead to vesicles with higher wall thickness.

Both f and M_n parameters are responsible of the morphologies reached by self-assembly of the block copolymers, as was previously described by Eisenberg and coll. (Mai and Eisenberg 2012). Some scaling relations have been determined between these parameters and geometric characteristics of the nanostructures; but these studies were made from diblock copolymers (Zhang and Eisenberg 1996). It has been indicated that triblock hydrophobic-hydrophilic-hydrophobic copolymers are similar to diblock copolymers in that there is only one molecular conformation that can lead to membrane formation: the hydrophobic chain ends must assemble into a membrane and the hydrophilic block must form a loop (U-shape) (LoPresti et al. 2009). Thus, our triblock copolymer could form polymersomes with the ordering of the macromolecular chain arrangement proposed in Scheme 3.

Multiblock copolymers as well as the nanostructures obtained from them have found an increasing interest from both the fundamental and applied points of view, especially
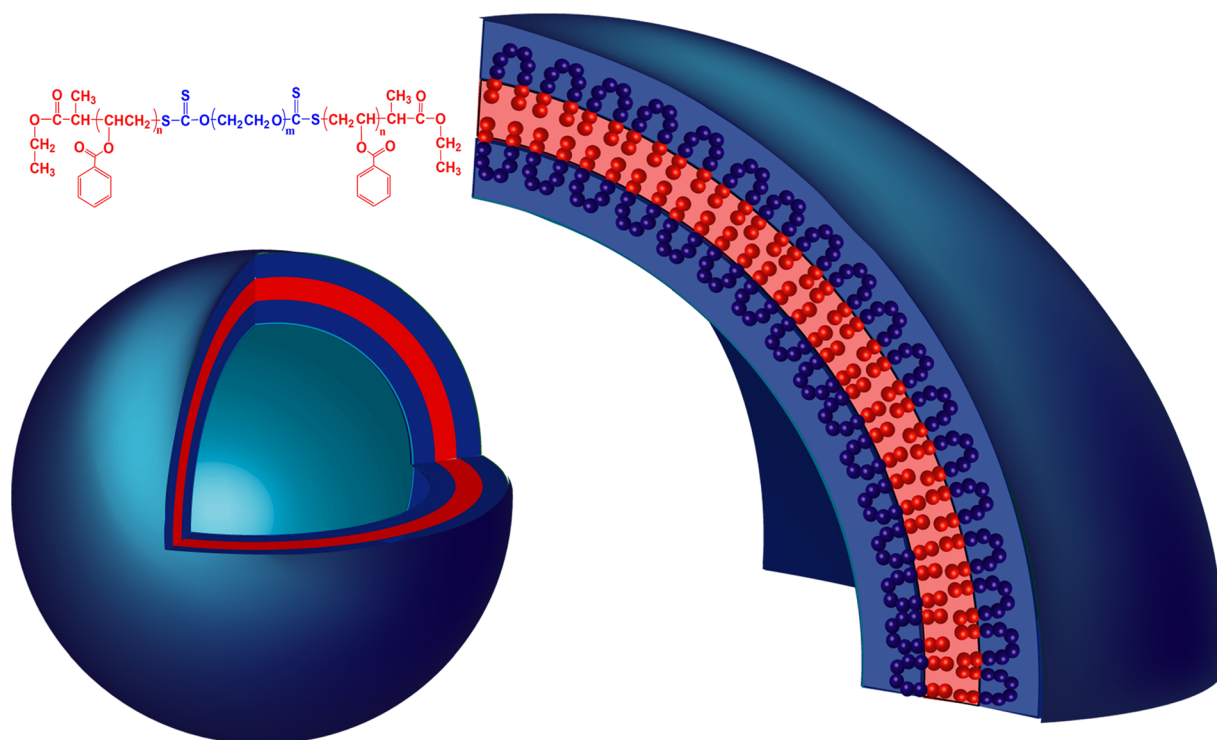

Fig. 6 SAXS curves of ferrocene-loaded samples and calculated scattering obtained from the polydisperse spherical shell particle model. Curves were displaced for clarity

Scheme 3 Schematic representation of the polymersome and macromolecular chain arrangement

in the biomedical area. ABA triblock polymersomes may offer further advantages, particularly with respect to controlling membrane transport and encapsulation (Bain et al. 2015). In particular, these researchers develop a method for the production of magnetopolymersomes based on poly(2-methyloxazoline)–poly(dimethylsiloxane)–poly(2-methyloxazoline), PMOXA-PDMS-PMOXA. The free radical polymerization of the methacrylate end groups of the PMOXA-PDMS-PMOXA triblock copolymer in the vesicular aggregates leads to the formation of polymer nanocapsules (Nardin et al. 2000). This change in chemistry, degree of polymerization, and membrane structure should give rise to better encapsulation and maintenance of the polymersome core contents (due to decreased permeability), along with the ability to stabilize and functionalize the vesicle by adaptation of reactive end groups (Bain et al. 2015). Therefore, these works allow to glimpse the advantages that new triblock copolymers could offer over diblock copolymers and promote future research.

Cytotoxicity studies

In order to evaluate the possible cytotoxicity of the polymersomes, we carried out a test of cell viability.

For that, raw macrophages cells were exposed to the polymersomes (10 and 50 µg/ml) during 48 hs through a MTT assay, which was compared with untreated (control) or LPS-treated cells. Macrophages act as the first line of defense in infections during host immune response, releasing pro-inflammatory cytokines such tumor necrosis factor (TNFa) and interleukin (IL1) (Cortizo et al. 2012).

When 10 µg/ml LPS was added to the culture medium as a positive control of cytotoxicity, a statistically significant ($p < 0.001$) inhibition of cell viability was detected after 48 hs of culture (Fig. 7). On the other hand, no significant differences in cell viability compared to the control cells were found when cell growth were in the presence of either 10 or 50 µg/mL polymersomes.

These findings suggest that PVBz-*b*-PEGX-*b*-PVBz-based polymersomes did not show any negative effect on the cellular viability and thus they seem not to induce cytotoxicity during the periods of time tested. These results could be attributed to the hydrophilicity of polyethylene glycol (PEG) which conform the outer layer of the polymersomes. Some research showed that in water solution, each subunit is associated with two or three water molecules (Branca et al. 2002). This bound
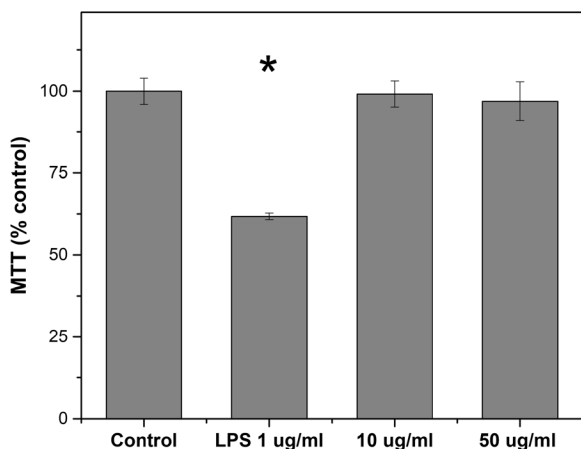
Fig. 7 Raw 264.7 cells viability in presence of polymersomes (10 and 50 μg/ml) during 48 hs. Ten micrograms per milliliter were used as positive control of cytotoxicity. *$p < 0.001$

hydration shell prevents the interaction of the vesicles with the surrounding and thereby limiting adverse immunological effects. Similar behavior has been demonstrated for polymersomes composed of other amphiphilic copolymers with highly hydrophilic part (Scherer et al. 2016), as well as the protective effect of PEG on pegylated drugs and pegylated nanocarriers (Harris and Chess 2003; Torchilin 2012).

Conclusions

In this work, several amphiphilic triblock copolymers (PBzV-b-PEG-b-PBzV) were synthesized by RAFT polymerization starting of previously derived PEG as a xanthate functional macroinitiator. The structure of these materials was confirmed by spectroscopic and chromatographic methodologies. Two copolymers, with $f \approx 35 \pm 10\%$, produced polymersomes by self-assembly through the solvent injection method. TEM analysis of these nanostructures shows diameters of 38.3 ± 0.3 nm and 22.5 ± 0.7 nm and narrow size distribution. Hydrodynamic diameters approximately three times higher than those observed by TEM were obtained by DLS measurements, as was expected considering the hydrophilic crown of the polymersomes. The analysis based on the SAXS measurements confirms the vesicle structures according the molecular weight of the starting triblock copolymers.

The in vitro results show that RAW 264.7 macrophages cultured in presence of polymersomes do not induce cytotoxicity during the evaluated culture periods.

Our results suggest that the new polymersomes are promising candidates as drug nanocarriers and drug delivery.

Compliance with ethical standards

Conflict of interest The authors declare that they have no conflicts of interests.

References

Alibolandi M, Ramezani M, Abnous K, Sadeghi F, Hadizadeh F (2015) Comparative evaluation of polymersome versus micelle structures as vehicles for the controlled release of drugs. J Nanopart Res 17:76–91

Bain J, Berry ME, Dirks CE, Staniland SS (2015) Synthesis of ABA tri-block co-polymer magnetopolymersomes via electroporation for potential medical application. Polymers 7: 2558–2571

Blanazs A, Armes SP, Ryan AJ (2009) Self-assembled block copolymer aggregates: from micelles to vesicles and their biological applications. Macromol Rapid Commun 30:267–277

Branca C, Magazù S, Maisano G, Migliardo F, Migliardo P, Romeo G (2002) Hydration study of PEG/water mixtures by quasi elastic light scattering, acoustic and rheological measurements. J Phys Chem B 106:10272–10276

Brinkhuis RP, Rutjes FPJT, van Hest JCM (2011) Polymeric vesicles in biomedical applications. Polym Chem 2:1449–1462

Christian DA, Cai S, Bowen DM, Kim Y, Pajerowski JD, Discher DE (2009) Polymersome carriers: from self-assembly to siRNA and protein therapeutics. Eur J Pharm Biopharm 71: 463–474

Colley HE, Hearnden V, Avila-Olias M, Cecchin D, Canton I, Madsen J, MacNeil S, Warren N, Hu K, McKeating JA, Armes SP, Murdoch C, Thornhill MH, Battaglia G (2014) Polymersome-mediated delivery of combination anticancer therapy to head and neck cancer cells: 2D and 3D in vitro evaluation. Mol Pharm 11:1176–1188

Cortizo AM, Ruderman G, Correa G, Mogilner IG, Tolosa EJ (2012) Effect of surface topography of collagen scaffolds on cytotoxicity and osteoblast differentiation. J Biomater Tissue Eng 2:125–132

Davidson GS, Terbrugge KG (1995) Histologic long-term follow-up after embolization with polyvinyl alcohol particles. Am J Neuroradiol 16:843–846

Discher DE, Ahmed F (2006) Polymersomes. Annu Rev Biomed Eng 8:323–341

Discher DE, Eisenberg A (2002) Polymer vesicles. Science 297: 967–973

García-Juan H, Nogales A, Blasco E, Martínez JC, Šics I, Ezquerra TA, Piñol M, Oriol L (2016) Self-assembly of thermo and light responsive amphiphilic linear dendritic block copolymers. Eur Polym J 81:621–633

Gradzielski M, Langevin D, Magid L, Strey R (1995) Small-angle neutron scattering from diffuse interfaces. 2. Polydisperse shells in water-n-alkane-C10E4 microemulsions. J Phys Chem 99:13232–13238

Guinier AF, Fournet G (1955) Small angle scattering of X-rays. Wiley, New York

Habel J, Ogbonna A, Larsen NW, Cherré S, Kynde S, Midtgaard SR, Kinoshita K, Krabbe S, Jensen GV, Hansen JS, Almdal K, Helix-Nielsen C (2015) Selecting analytical tools for characterization of polymersomes in aqueous solution. RSC Adv 5:79924–79946

Harris JM, Chess RB (2003) Effect of pegylation on pharmaceuticals. Nat Rev Drug Discov 2:214–221

Johnston AH, Dalton PD, Newman TA (2010) Polymersomes, smaller than you think: ferrocene as a TEM probe to determine core structure. J Nanopart Res 12:1997–1200

Kline SR (2006) Reduction and analysis of SANS and USANS data using IGOR pro. J App Crystallography 39:895–900

Labruère R, Sicard R, Cormier R, Turos E, West L (2010) Poly(vinyl benzoate) nanoparticles for molecular delivery: studies on their preparation and in vitro properties. J Control Release 148:234–240

Lastra ML, Molinuevo MS, Cortizo AM, Cortizo MS (2017) Fumarate copolymer-chitosan cross-linked scaffold directed to osteochondrogenic tissue engineering. Macromol Biosci 17. https://doi.org/10.1002/mabi.201600219

Lee JS, Feijen J (2012) Polymersomes for drug delivery: design, formation and characterization. J Control Release 161:473–483

Li Z, Tan BH (2014) Towards the development of polycaprolactone based amphiphilic block copolymers: molecular design, self-assembly and biomedical applications. Mat Sci Eng C 45:620–634

Lipscomb CE, Mahanthappa MK (2009) Poly(vinyl ester) block copolymers synthesized by reversible addition-fragmentation chain transfer polymerizations. Macromolecules 42:4571–4579

Lipscomb CE, Mahanthappa MK (2011) Microphase separation mode-dependent mechanical response in poly(vinyl ester)/PEO triblock copolymers. Macromolecules 44:4401–4409

Liu G, Ma S, Li S, Cheng R, Meng F, Liu H, Zhong Z (2010) The highly efficient delivery of exogenous proteins into cells mediated by biodegradable chimaeric polymersomes. Biomaterials 31:7575–7585

Lopez-Oliva AP, Warren NJ, Rajkumar A, Mykhaylyk OO, Derry MJ, Doncom KEB, Rymaruk MJ, Armes SP (2015) Polydimethylsiloxane-based diblock copolymer nano-objects prepared in nonpolar media via RAFT-mediated polymerization-induced self-assembly. Macromolecules 48: 3547–3555

LoPresti C, Lomas H, Massignani M, Smart T, Battaglia G (2009) Polymersomes: nature inspired nanometer sized compartments. J Mater Chem 19:3576–3590

Mai Y, Eisenberg A (2012) Self-assembly of block copolymers. Chem Soc Rev 41:5969–5985

Meng F, Zhong Z (2011) Polymersomes spanning from nano- to microscales: advanced vehicles for controlled drug delivery and robust vesicles for virus and cell mimicking. J Phys Chem Lett 2:1533–1539

Mosqueira VC, Legrand P, Gulik A, Bourdon O, Gref R, Labarre D, Barratt G (2001) Relationship between complement activation, cellular uptake and surface physicochemical aspects of novel PEG-modified nanocapsules. Biomaterials 22: 2967–2979

Nardin C, Hirt T, Leukel J, Meier W (2000) Polymerized ABA triblock copolymer vesicles. Langmuir 16:1035–1041

Onaca O, Enea R, Hughes DW, Meier W (2009) Stimuli-responsive polymersomes as nanocarriers for drug and gene delivery. Macromol Biosci 9:129–139

Pippa N, Pispas S, Demetzos C (2016) Polymer self-assembled nanostructures as innovative drug nanocarrier platforms. Curr Pharm Des 22:2788–2795

Roy D, Sumerlin BS (2011) Block copolymerization of vinyl ester monomers via RAFT/MADIX under microwave irradiation. Polymer 52:3038–3045

Scherer M, Kappel C, Mohr N, Fischer K, Heller P, Forst R, Depoix F, Bros M, Zentel R (2016) Functionalization of active Ester-based polymersomes for enhanced cell uptake and stimuli-responsive cargo release. Biomacromolecules 17: 3305–3317

Torchilin VP (2012) Multifunctional nanocarriers. Adv Drug Deliv Rev 64:302–315

Woodle MC (1995) Sterically stabilized liposome therapeutics. Adv Drug Deliv Rev 16:249–265

Working PK (1997) Safety of poly(ethylene glycol) and poly(ethylene glycol) derivatives. In Poly(ethylene glycol)chemistry and biological applications, eds Harris JM, Zalipsky S, (ACSC, Symposium Series 680) Ch 4, pp 45–57

Yamaoka T, Tabata Y, Ikada Y (1994) Distribution and tissue uptake of poly(ethylene glycol) with different molecular weights after intravenous administration to mice. J Pharm Sci 83:601–606

Zelikin AN, Price AD, Stadler B (2010) Poly(methacrylic acid) polymer hydrogel capsules: drug carriers, sub-compartmentalized microreactors, artificial organelles. Small 6:2201–2207

Zhang L, Eisenberg A (1996) Multiple morphologies and characteristics of "crew-cut" micelle-like aggregates of polystyrene-b-poly(acrylic acid) diblock copolymers in aqueous solutions. J Am Chem Soc 118:3168–3181